Published in final edited form as:

Synapse. 2013 May ; 67(5): 205–215. doi:10.1002/syn.21632.

Golgi Phosphoprotein 4 (GPP130) is a Sensitive and Selective Cellular Target of Manganese Exposure

Melisa Masuda[1], **Michelle Braun-sommargren**[2], **Dan Crooks**[3], and **Donald R. Smith**[1,*]

[1]Department of Microbiology and Environmental Toxicology, University of California, 1156 High Street, Santa Cruz, California 95064

[2]Locus Development, Inc, 458 Brannan Street, San Francisco, California 94107

[3]Molecular Medicine Program, Eunice Kennedy Shriver National Institute of Child Health and Human Development, Bethesda, Maryland 20892

Abstract

Chronic elevated exposure to manganese (Mn) is associated with neurocognitive and fine motor deficits in children. However, relatively little is understood about cellular responses to Mn spanning the transition between physiologic to toxic levels of exposure. Here, we investigated the specificity, sensitivity, and time course of the Golgi Phosphoprotein 4 (GPP130) response to Mn exposure in AF5 GABAergic neuronal cells, and we determined the extent to which GPP130 degradation occurs in brain cells in vivo in rats subchronically exposed to Mn. Our results show that GPP130 degradation in AF5 cells was specific to Mn, and did not occur following exposure to cobalt, copper, iron, nickel, or zinc. GPP130 degradation occurred without measurable increases in intracellular Mn levels and at Mn exposures as low as 0.54 μM. GPP130 protein was detectable by immunofluorescence in only ~15–30% of cells in striatal and cortical rat brain slices, and Mn-exposed animals exhibited a significant reduction in both the number of GPP130-positive cells, and the overall levels of GPP130 protein, demonstrating the in vivo relevance of this Mn-specific response within the primary target organ of Mn toxicity. These results provide insight into specific mechanism(s) of cellular Mn regulation and toxicity within the brain, including the selective susceptibility of cells to Mn cytotoxicity.

Keywords

neurotoxicity; GABAergic; manganese; rodents; AF5 cells; homeostasis

INTRODUCTION

Manganese (Mn) is a transition metal that serves as a cofactor for numerous enzymes, and is essential for many biological processes, including brain development (Keen, 1984; Prohaska, 1987). At elevated exposures, however, Mn can accumulate widely throughout the

*Correspondence to: Donald R. Smith, Department of Microbiology and Environmental Toxicology, University of California, 1156 High Street, Santa Cruz, CA 95064, USA. drsmith@ucsc.edu.

brain and act as a neurotoxin (Criswell et al., 2012; Reaney et al., 2006), leading to deficits in cognitive and motor function (Aschner et al., 2005; Kern et al., 2010; Lucchini et al., 1999, 2011). The specific mechanisms leading to these functional deficits are not well-understood, though Mn has been shown to target dopaminergic and GABAergic neurons in the basal ganglia and elsewhere (Crooks et al. 2007a,b; Gwiazda et al., 2002; Stanwood et al., 2009). For example, Stanwood et al. (2009) reported Mn cytotoxicity in dopaminergic and GABAergic neurons exposed in vitro to 10–800 μM Mn, with levels of 100 μM Mn leading to increased cytoskeletal abnormalities and changes in neurite length and integrity. Using a GABAergic AF5 neuronal cell model, Crooks et al. (2007a,b) reported altered cellular metabolism in response to Mn exposure, including increased intracellular GABA and disrupted cellular iron homeostasis at exposure levels of 25–300 μM Mn. While these studies illuminate the pathophysiology of Mn neurotoxicity at elevated exposures (Racette et al., 2012), relatively little is understood about cellular responses to Mn exposures that only slightly exceed physiologic levels, a scenario of importance for more fully understanding the risks from environmental exposure.

The transition from physiologic to toxic cellular Mn levels likely occurs when homeostatic influx/efflux processes become imbalanced. Cellular Mn uptake/influx into brain cells occurs via divalent metal transporter-1 (DMT1), transferrin receptor (TfR), and voltage regulated and store-operated Ca2+ channel mechanisms (Davidsson et al., 1989; Gunshin et al., 1997; Lucaciu et al., 1997; Riccio et al., 2002). However, comparatively little is known about the mechanisms of cellular Mn efflux from cells in the brain. Ferroportin, SPCA (secretory pathway Ca2+ Mn2+ ATPases), and ATP13A2 have all been implicated to facilitate cellular Mn efflux (Leitch et al., 2011; Madejczyk and Ballatori, 2012; Tan et al., 2011; Yin et al., 2010). ATP13A2 may transport Mn into lysosomes and thus may also mediate Mn trafficking in the neuron (Tan et al., 2011).

SPCA1 is a Golgi trans-membrane protein in the brain capable of transporting Mn into the Golgi lumen with high affinity (Sepulveda et. al., 2009). Studies by Leitch et al. (2011) showed that SPCA1 knock down in hepatocyte derived (WIF-B) cells led to an increase in Mn specific cell death, whereas over expression of SPCA1 in human embryonic kidney cells (HEK-293T) protected cells against Mn toxicity. Similarly, Mukhopadhyay et al. (2010) reported that increased activity of SPCA1 led to increased Mn transport into the Golgi and decreased Mn cytotoxicity in HeLa cells, while blocking Mn transport into or out of the Golgi increased cytotoxicity, suggesting that the Golgi may play an important role in Mn homeostasis and detoxification in HeLa cells.

Additionally, Mukhopadhyay et al. (2010) reported that elevated (500 μM) exposure and uptake of Mn into the Golgi of HeLa cells led to the lysosomal degradation of the cis-Golgi associated transmembrane protein Golgi Phosphoprotein 4 (GPP130; gene GOLIM4). Notably, blocking Mn uptake into the Golgi protected against GPP130 degradation, suggesting GPP130 may also play a role in cellular Mn homeostasis (Mukhopadhyay et al., 2010). Although the cellular functions of GPP130 are not fully understood, GPP130 has been shown to mediate the cellular trafficking of protein cargo directly from endosomes to the Golgi apparatus via a pathway that bypasses late endosomes and pre-lysosomes (Puri et al., 2002). By utilizing this bypass pathway, proteins and toxins are able to avoid lysosomal

degradation and are able to exhibit their effects by trafficking to the Golgi (Mukhopadhyay et al., 2010). Knockdown of GPP130 leads to increased cycling of endosomal proteins between the cell surface and endosomes (Linstedt et al., 1997; Natarajan and Linstedt, 2004). The relationship between Mn and GPP130 within neuronal cells, including the extent to which Mn versus other divalent cations specifically elicits GPP130 degradation within brain cells in vivo, is not known.

The objectives of this study were two-fold: (i) explore the specificity, sensitivity, and time course of the GPP130 response to Mn exposure in AF5 GABAergic neuronal cells; and (ii) determine the extent to which GPP130 degradation occurs in brain cells in vivo in rats subchronically exposed to Mn. Our results show that GPP130 degradation is specific to Mn in AF5 cells, and does not occur following exposure to cobalt, copper, iron, nickel, or zinc. GPP130 degradation occurs rapidly (<1 h post Mn exposure) and at Mn exposures as low as 0.54 μM, which are ~200-times lower than exposures previously reported to result in GPP130 degradation (Mukhopadhyay et al., 2010). Furthermore, GPP130 protein was detected in only ~15–30% of striatal and cortical brain cells in control animals, and Mn-exposed animals exhibited a significant reduction in both the number of GPP130-postive cells, and the overall levels of GPP130 protein, demonstrating the in vivo relevance of this Mn-specific response within the predominant target organ of Mn toxicity. These results provide insight into novel mechanisms of cellular Mn regulation and toxicity within the brain.

MATERIALS AND METHODS

Cell culture

The immortalized mesencephalic-derived AF5 cell line was a generous gift provided by Dr. W.J. Freed of NIH/NIDA. For all experiments utilizing the AF5 cell line, cells were grown to confluence in T75 flasks in Dulbecco's Modified Eagle Medium (DMEM; Gibco Life Technologies, Gaithersburg, Md.) containing 10% fetal bovine serum (FBS; Gibco Life Technologies, Gaithersburg, Md.) and 100 μg/mL streptomycin (Bio-Whittaker, Walkersville, Md.), and maintained in a 37°C humidified environment in a 5% CO_2 incubator. Cells were split into either 6-well plates or T25 flasks and grown to 80% confluence, then differentiated for 4 days post 80% confluence in Neurobasal-A medium with 10% FBS, 2% B-27 serum-free growth supplement (B-27, Gibco Life Technologies, Gaithersburg, Md.) and 1.25% 200mM L-Glutamine (Gibco Life Technologies, Gaithersburg, Md.). For metal treatments, Neurobasal medium was removed and replaced with Neurobasal medium spiked with the indicated metal concentrations for exposure durations ranging from 1 to 24 h, depending on the experiment. The actual metal concentrations in control and exposure medium were determined using a Finnigan MAT Element high resolution inductively coupled plasma – mass spectrometer (ICP-MS), as described below. Following treatment, cells were harvested by trypsinization and collected for analysis by centrifugation at 1,000 × *g* for 10 min; cell pellets were frozen at −80°C until further analysis. Lysate protein concentrations were determined using the Pierce BCA Protein Assay Kit (Thermo Fisher Scientific, Rockford, IL), following the manufacturers instructions.

Immunoblot analysis

AF5 cell pellets were lysed in RIPA buffer (pH 7.4) and sonication, and lysates were adjusted to identical total protein concentrations following measurement of total lysate protein levels using the BCA assay. Cell lysate protein (20 μg per lane) and the molecular weight marker (10 μg) were separated by SDS-PAGE on a 4–12% Bis-Tris gel (Novex; Invitrogen Life Technologies, Gaithersburg, Md.) and transferred to a PVDF membrane. Membranes were blocked in 5% nonfat dry milk tris-buffered saline (pH 8.3) and Tween (PlusOne Tween 20; GE Healthcare Life Sciences, Pittsburgh, PA) (TBST, pH 7.4) overnight at 4°C. Membranes were incubated with GPP130 primary antibody (Anti-GOLPH4, ab28049, Abcam, Cambridge, UK; 1:1000) or anti-β-tubulin as a loading control (ab6046; Abcam, Cambridge, UK; 1:1000) for 1 hour, washed in TBST, and then incubated with secondary antibody (bovine anti-rabbit IgG-HRP, sc-2370; Santa Cruz Biotech, Santa Cruz, CA; 1:1000) for 1 h. The membranes were visualized using ECL Plus (GE Healthcare Life Sciences, Pittsburgh, PA) and imaged using a Typhoon Fluorescent Scanner. The protein bands were analyzed using ImageQuant. Beta-tubulin band densities were not measurably different across lanes or treatment condition, indicating comparable protein loading across gel lanes (consistent with protein lysate levels measured by BCA), and no Mn effect on cellular β-tubulin levels.

Intracellular Mn concentration measurement

Cellular Mn levels were measured using trace metal clean methods as previously described (Crooks et. al., 2007a, b; Kwik-Uribe et al., 2003). Briefly, AF5 cells were harvested by trypsinization, and the pellets were washed once with phosphate buffered saline (PBS, pH 7.4) supplemented with 10 mM ethylenediaminetetraacetic acid (EDTA; Gibco Life Technologies, Gaithersburg, Md.), followed by a second wash with PBS alone to remove surface-associated Mn from the cells. Cell pellets were digested using 100 μL 1N nitric acid and heated on a heat block at 80°C for 30 min. The digestate was diluted using Milli-Q water for analyses of total intracellular Mn levels using a Thermo XR-ICP-MS, measuring masses ^{55}Mn (medium resolution) and ^{103}Rh, the latter as an internal standard. Manganese concentrations were determined by external standardization using certified standards (Inorganic Ventures, Christiansburg, VA). The analytical detection limit for Mn analyses was 0.01 ng/mL.

Animals and Mn treatment

Adult female Long Evans (*Rattus Norvegicus*) rats, weighing between 270 and 350 g, were dosed with either control vehicle (n=3) or 9.6 mg Mn/kg (n=3) by intraperitoneal (i.p.) injection, once a day, 3 days a week, for a duration of 4 weeks. A Mn stock solution of 49.6 mg/mL was prepared using $MnCl_2$-hexahydrate diluted in Milli-Q water, and subsequently diluted to 6.7 mg/mL and filter sterilized for delivery to the animals. Manganese concentrations in the dosing solutions were routinely verified by atomic absorption spectrometry. This Mn exposure regimen was selected based on prior studies in our lab showing it was well-tolerated but produced subtle neurochemical and neuromotor deficits (Gwiazda et. al., 2005). All animal care and treatments were approved by the institutional

IACUC, and adhered to NIH guidelines set forth in the Guide for the Care and Use of Laboratory Animals (NRC, 2011).

Perfusion and blood and tissue collection

Twenty-four hours after the final dose was administered, the rats were sacrificed by i.p. injection with 75 mg/kg pentobarbital, followed immediately by collection of whole blood via cardiac puncture, and in situ brain fixation via upper body perfusion through the heart with ice cold 4% paraformaldehyde (PFA). The brain was removed and immediately immersed in 4% PFA and fixed for 12 h at 4°C. The solution was changed to a 10% sucrose solution and fixed for 24 h at 4°C, and then the solution was changed again to a 30% sucrose solution for 48 h at 4°C. Whole brains were then embedded in freezing medium and stored at −70°C.

Immunohistochemistry

Immunohistochemical (IHC) analysis was performed in cortical and striatal brain regions, as previously described (Kern et al., 2010). Briefly, PFA-fixed brains were sectioned coronally in 20 μm slices at −20°C using a cryotstat (Leica Microsystems, model CM30505). Slices containing dorsal striatum and S1 dysgranular zone cortex (Bregma 0.48 mm, Paxinos and Watson, 1998) were mounted on Superfrost/Plus slides, with three slices per animal per treatment on each slide (i.e., six brain slices per slide balanced by treatment) and stored at −20°C. Six brain slices per animal per treatment group for the cortex and one representative brain slice per animal per treatment for the striatum were analyzed for GPP130 by IHC.

For immunostaining, mounted brain slices were blocked with 4% normal goat serum and permeablized with 0.1% Triton X-100 (Sigma-Aldrich) for 1 h. Tissues were then washed three times with PBS, and incubated with primary antibody (Anti-GOLPH4, ab28049; Abcam, Cambridge, UK) (1:1000) overnight at 4°C. Tissues were then washed with PBS, phosphate buffered saline Tween (PBST, pH 7.4), and incubated with secondary antibody (goat anti-rabbit IgG, Alexa Fluor 488; Molecular Probes). Slides were washed again with PBST and stained for 10 min with Draq5 (4084; Cell Signaling Technology, Beverly, MA), followed by a final washing with PBS. Slides were then loaded with Fluoromount GTM (Southern Biotech) and cover-slipped prior to analyses by confocal microscopy.

Confocal microscopy

Immunostained brain slices were analyzed using a Zeiss LSM PASCAL confocal microscope. Images were captured and exported using AIM software version 4.2. (Carl Zeiss, Germany). All images on each slide were taken with constant settings at either ×20 or ×63 magnification using the same detector gain and amplifier offset settings within each magnification for fluorescent image comparison. The ×20 images were taken from two separate fields per brain region per brain slice, while the ×63 images were - taken from 10 separate fields per brain region per slice. GPP130 staining in brain slices was quantified using both ×20 and ×63 magnification for two reasons. First, the ×20 magnification provided assessment of a larger number of cells per field for analyses, but with higher fluorescence background levels and thus reduced resolution for detection of cellular GPP130 fluorescence. Second, images at the higher ×63 magnification were collected because this

magnification level provided substantially reduced background tissue fluorescence within each field and substantially improved resolution of cellular GPP130 staining, thereby improving the detection threshold for identifying GPP130-positive cells.

Image analysis and quantification

Brain slices per region per animal were qualitatively scored for protein fluorescence as previously described (Kern et. al 2010). A total of six (×20 cortex) or one (×63 cortex and ×63 striatum) immunostained brain slice(s) per brain region per animal per treatment were analyzed for GPP130. For the ×20 images, a total of 36 fields/treatment for the cortex were qualitatively scored for protein (based on two fields per brain region × six brain slices per animal × three animals per treatment). For the ×63 images a total of 30 fields/treatment for the striatum (based on 10 fields per brain region × one representative brain slice per animal × one representative animal per treatment) were quantified and analyzed for treatment-based comparisons of fluorescent density within each slide using Metamorph software (MetaXpress, multiwavelength cell scoring and count nuclei module; Molecular Devices Corporation). For these analyses total grayscale values (pixel brightness) were obtained by summing all of the grayscale values for all objects detected above the defined threshold for each slide. Fluorescence density in the Mn-treated animals was compared with that of control animals within each slide to determine Mn effects. Threshold limits were set by analyzing three fields/brain over three brain slices/animal and identifying the cells that were considered to be positive. From this, the Approximate Minimum Width, Approximate Maximum Width, and Intensity Above Local Background settings were adjusted and set to capture and identify all cells that were determined to be positive within a given field; these settings were 3 μm, 15 μm, and 80 gray/level, respectively.

Statistical analysis

Treatment comparisons were made using t-test or analysis of variance (ANOVA) and Dunnett's or Tukey's post hoc tests. *P*-values of <0.05 were considered statistically significant. All analyses were conducted using JMP software (Version 9.0; SAS Institute).

RESULTS

GPP130 degradation in AF5 cells is Mn-specific

In order to provide insight into the cellular regulation of Mn and/or the mechanism of cellular Mn toxicity, we investigated whether GPP130 degradation in AF5 cells was Mn-specific, or if GPP130 degradation also occurred with other divalent metal treatments. Results show that Mn exposure (150 μM) led to >80% reduction in cellular GPP130 protein levels, while exposure to Ni, Zn, Co (all 150 μM), and Fe (300 μM) had no measurable effect, based on ANOVA ($F(6, 14)=73.3$, $P<0.0001$) and Dunnett's post hoc test (Fig. 1). Interestingly, treatment with 150 μM Cu led to a small (~17%) but statistically significant increase in GPP130 protein levels, compared to control. These results demonstrate that the effect of metal exposure on GPP130 degradation, at metal levels that do not cause measurable overt cytotoxicity (Crooks et al., 2007b), is highly Mn-specific.

GPP130 degradation in AF5 cells is stimulated by Mn even in the absence of measurable changes in intracellular Mn concentration

To elucidate the sensitivity of the GPP130 response to Mn over the transition from physiologic to supraphysiologic intracellular Mn levels, AF5 cells were treated with a range of physiologically relevant and sub-toxic Mn concentrations. Results show a significant effect of Mn treatment on cellular GPP130 levels (ANOVA $F(5, 13) = 140$, $P<0.0001$), with significant cellular GPP130 degradation (~50% reduction) occurring at the lowest Mn exposure level explored here (0.54 μM) (Fig. 2a), even though total intracellular Mn concentrations did not measurably increase until Mn exposure levels in the medium reached 140 μM (ANOVA $F(5, 36) = 41.2$, $P<0.0001$; Fig. 2b). Note, however, that there were trending but nonsignificant (P=~0.1) increases in intracellular Mn levels at the 5.3 and 27 μM exposure levels. This indicates that GPP130 degradation is highly sensitive to Mn exposure, occurring at exposure levels below those that produce measureable increases in intracellular Mn.

GPP130 degrades rapidly over time in parallel with a rapid increase, then decrease in intracellular Mn concentrations

To evaluate the rapid temporality of the GPP130 response to Mn exposure, AF5 cells were treated with sub-toxic Mn concentrations for durations of 1, 2, 4, 8, or 24 h. Significant GPP130 degradation can be seen in cells treated with 5.4 μM Mn (~15% reduction) and 140 μM Mn (~25% reduction) as early as 1 hour post Mn exposure, the earliest time point evaluated here (Fig. 3a; ANOVA for Mn treatment, exposure duration, and Mn treatment × exposure duration interaction, $F(2, 35) = 575$, $F(4,35) = 119$, and $F(8,35) = 33.0$, respectively, P's<0.0001 for all). Notably, intracellular Mn levels significantly increased over the first 2 hours of exposure in both the 5.4 and 140 μM treatments, and then significantly decreased over the subsequent 22 h (h 2–24 of exposure) even in the presence of continued Mn exposure (Fig. 3b; ANOVA for Mn treatment, exposure duration, and Mn treatment×exposure duration interaction, $F(2, 46) = 730$, $F(4,46) = 60.1$, and $F(8, 46) = 31.8$, respectively, P's<0.0001 for all). The close temporal association between changes in intracellular Mn levels (rapid increase, then decrease) with GPP130 degradation suggests a possible role for GPP130 in cellular Mn homeostasis (e.g., loss of GPP130 favors cellular Mn efflux).

GPP130 rate of recovery is slower than the rate of disappearance following Mn exposure

Cellular GPP130 degradation occurs rapidly (see above) via the lysosome (Mukhopadhyay et al., 2010), though the rate of recovery of cellular GPP130 levels following cessation of Mn exposure is not known. Here, AF5 cells were exposed to control (0.09 μM), 5.4 μM, or 140 μM Mn for 8 h, and then allowed to recover in control medium for the subsequent 16 h. Results show significant degradation of GPP130 by 8 h in the 5.4 μM and 140 μM treatments (to ~40% and 25% of control, respectively), with small but significant increases (recovery) in cellular GPP130 levels by 24 h (to ~55% and 45% of control, respectively) (Fig. 4a; ANOVA for Mn treatment, recovery time, and Mn treatment×recovery time interaction, $F(2,15) = 478$, $F(1,15) = 49.3$, and $F(2, 15) = 13.0$, respectively, P's<0.001 for all). Notably, the apparent rate of GPP130 recovery after the cessation of Mn exposure was

nearly identical in both the 5.4 μM and 140 μM treatment groups. In parallel, intracellular Mn levels increased significantly after 8 hours exposure to 140 μM Mn, which then rapidly and significantly declined after cessation of Mn exposure over the subsequent 16 h; in contrast, intracellular Mn levels were not measurably increased after 8-h exposure to 5 μM Mn, nor did levels measurably change after cessation of exposure (Fig. 4b; ANOVA for Mn treatment, recovery time, and Mn treatment × recovery time interaction, $F(2, 15) = 101$, $F(1,15) = 65.9$, and $F(2, 15) = 38.1$, respectively, P's<0.0001 for all). These data indicate that recovery of cellular GPP130 levels following cessation of Mn exposure is incomplete and temporally much slower compared with the initial degradation response to Mn.

GPP130 degradation occurs in vivo in response to Mn and may be cell specific

We explored whether sub-chronic Mn exposure in rats resulted in reductions in brain GPP130 protein levels using an exposure regimen (9.6 mg/kg/d × 3 days/week × 4 weeks via i.p. injection) shown previously to produce subtle asymptomatic neurotoxic effects (Gwiazda et. al., 2005). First, it is noteworthy that only ~20–30% of Draq5-identified cells in the S1 dysgranular zone of the cortex and 10–20% in the dorsal striatum of control animals were identified as GPP130 positive (see Materials and Methods for detection threshold criteria) (Table I, Fig. 5). Second, we detected no significant difference in the total number of cell nuclei via Draq5 staining in either the cortex or dorsal striatum of control versus Mn-treated animals (Table I; $P>0.2$, t-test). However, there was a significant reduction in the percent of cells identified as GPP130-positive in Mn-treated animals, with ~20–30% of cells identified as GPP130-positive in the S1 dysgranular zone of the cortex of control animals compared with <10% in Mn-treated animals ($P<0.001$, t-test). Similar differences between control and Mn-exposed animals occurred in the dorsal striatum (i.e., 10–20% GPP130-positive cells in controls versus 4–5% in Mn-treated animals, $P<0.05$, t-test) (Table I).

Further analyses show that Mn treatment reduced GPP130 protein levels in the cortex to ~15–42% of controls ($P<0.005$, t-test), based on analysis of total cellular fluorescence; there was a parallel reduction in the percent of GPP130-positive cells to ~23–40% of controls ($P<0.001$, t-test) (see Figs. 6a and 6b, "Total Fluorescence, All Cells"). Notably, however, in cells identified as GPP130-postive, total fluorescence in GPP130-positive cells was only slightly but nonsignificantly reduced in Mn-treated animals to ~90% of controls (see Figs. 6a and 6b, "Total Fluorescence in GPP-Positive Cells"), suggesting there exists a population of brain cells that do not exhibit a GPP130 degradation response to Mn.

We also analyzed GP130 protein fluorescence in cells identified as nonpositive for GPP130, since it is possible that some cells contained very low levels of GPP130 staining below the defined fluorescence threshold detection limits, and therefore were misclassified as nonpositive GPP130 cells. Our results show that Mn treatment significantly reduced GPP130 protein levels to 14–48% of controls in cells defined as GPP130 nonpositive (Figs. 6a and 6b), paralleling the Mn effect in GPP130 positive cells. This suggests that cells containing very low levels of GPP130 (defined "non-positive") are equally as responsive to Mn as cells identified as GPP130 positive.

We also evaluated whether dorsal striatal cells similarly responded to Mn exposure as cells in the cortex, since the striatum is a well-recognized target region for Mn neurotoxicity (Gwiazda et al., 2002, 2007; Kim et al. 2005). Our results show that Mn treatment reduced striatal GPP130 protein levels to 50% of controls (based on total cellular fluorescence), and reduced the number of GPP130-positive cells to 20% of control (Table II, t-test). It is noteworthy, however, that in the striatum, GPP130 staining appeared primarily on the surface of the cells, and was typically localized to cell processes (Fig. 5), compared to the cortex, where GPP130 staining appeared within the cell in a pattern suggesting Golgi localization (Fig. 5).

DISCUSSION

Our results in AF5 GABAergic cells show that GPP130 degradation was specific to Mn exposure, and not to other cationic metals such as Co, Ni, Zn, Cu, or Fe (Fig. 1). Since Co(II) is a biologic analog to Mn(II), while Fe(III) is an analog to Mn(III) (da Silva and Williams, 2001), this specificity suggests that GPP130 degradation in response to Mn is a physiological, as opposed to toxicological response. Consistent with this, studies in HeLa cells showed that only GPP130, and not GP73 (a related cis-Golgi protein), was degraded in response to Mn exposure (Mukhopadhyay et al., 2010). Mukhopadhyay et al. (2010) mapped the Mn-responsive region of GPP130 to its Golgi luminal stem domain; deletion of this stem domain led to a loss of GPP130 sensitivity to Mn and the displacement of GPP130 from the cis-Golgi towards the trans-Golgi network. Thus, although as yet there is no evidence of direct Mn binding or interaction with this domain, it is clear that the luminal stem domain of GPP130 confers Mn-sensitive responsiveness to the protein. We characterized both extracellular (exposure medium) and intracellular Mn concentrations in AF5 cell cultures so as to elucidate the sensitivity of the GPP130 response to Mn over the transition from physiologic to supra-physiologic intracellular Mn levels. The ~50% reduction in cellular GPP130 levels following 24 hr exposure to 0.54 μM Mn, the lowest Mn exposure level explored here, and the ~80% reduction following exposure up through 27 μM Mn occurred without measurable increases in total intracellular Mn concentrations (Fig. 2). A more detailed assessment of the temporal relationship between intracellular Mn concentrations and cellular GPP130 protein levels over the 24 hr exposure period showed that intracellular Mn levels actually increased over the first 2 hrs of exposure to 5.4 or 140 μM Mn in association with a rapid significant decrease in cellular GPP130 protein levels (Fig. 3). However, over the subsequent 22 hrs of exposure, intracellular Mn levels declined even in the presence of continued Mn exposure, while GPP130 protein levels continued to significantly decline (Fig. 3). This temporal association between changes in intracellular Mn levels (rapid increase, then decrease) with GPP130 degradation suggests a possible role for GPP130 in cellular Mn homeostasis, i.e., loss of GPP130 favors cellular Mn efflux.

The suggestion that loss of GPP130 favors cellular Mn efflux is consistent with a role for GPP130 protein in the transition of cellular Mn from physiologic to supra-physiologic. While systemic Mn is regulated largely through hepatocyte efflux of excess Mn into the bile (Bertinchamps et al., 1966), comparatively little is known about the mechanisms of Mn efflux from cells in the brain. Recent studies suggest that cellular Mn, like iron, may be effluxed by ferroportin, and that elevated exposure to Mn may induce ferroportin expression

in brain cells (Madejczyk and Ballatori, 2012; Yin et al., 2010.). Other cellular proteins, including secretory pathway Ca2+ Mn2+ ATPases (SPCA) and ATP13A2 have also been suggested to play a role in cellular Mn efflux (Leitch et al., 2011; Tan et al., 2011). SPCA1, a Golgi transmembrane protein, was shown to facilitate transport of intracellular Mn into the Golgi lumen; blocking Mn transport into or out of the Golgi led to increased cytotoxicity, supporting an important role of the Golgi in cellular Mn detoxification (Mukhopadhyay et al. 2010). Collectively, these data suggest that the Golgi, and SPCA1 and GPP130 in particular, play a role in cellular Mn homeostasis and resistance to elevated Mn exposures, including possibly cellular Mn efflux (Fig. 7).

Our results in rodents on GPP130 expression and response to Mn *in vivo* demonstrate that i) GPP130 protein appears to be robustly expressed in selective brain cells, and ii) Mn exposure produces significant reductions in cellular GPP130 protein levels in a subset of those cells. In control animals, only ~20 – 30% of Draq5-identified cells in the S1 dysgranular zone of the cortex and 10 – 20% of cells in the dorsal striatum were identified as GPP130-positive (Table I). Moreover, Mn exposure caused a ~50% to ~80% decrease in the number of GPP130-positive cells in both brain regions, which appears to account for the comparable decrease in total brain region GPP130 protein levels (Fig. 6, Table II). Supporting this suggestion, Metamorph analyses specifically of GPP130-postive cells in the cortex shows that GPP130 protein levels in those cells were only slightly but non-significantly reduced by ~10% in Mn-treated animals compared to controls (Fig. 6), in contrast to the ~80% decrease in GPP130 protein levels in Mn-treated AF5 cells (Fig. 2). These results suggest that there are different populations of GPP130-positive cells that differ in their GPP130 degradation response to Mn. Cells and regions within the brain are known to differ in susceptibility to elevated Mn exposure, although the basis for these differences in susceptibility are not well understood (Garrick et al. 2003; Gunter et al., 2006; Stanwood et al. 2009). Depending on the physiological role that GPP130 plays in relation to Mn, these results suggest that GPP130 may play a role in mediating cell-specificity of susceptibility/ resistance to elevated Mn exposure.

The lowest Mn exposure level used here (0.54 μM Mn) to elicit a GPP130 degradation response in AF5 cells was only ~6-fold higher than background Mn levels in the cell culture medium (0.09 μM Mn), and represents a relative increase in extracellular Mn levels that is well within the range of circulating Mn levels in humans (e.g., ~0.14–1.4 μM; Zota et al., 2009; Montes et al., 2008). Further, the intracellular Mn levels reported here for the control and Mn-treated AF5 GABAergic cells (i.e., 3.6–22 ng Mn/mg protein, Fig. 2b) are highly comparable to brain Mn levels in the control and Mn-treated rats (e.g., 3 and 16 ng Mn/mg brain protein; based on brain tissue Mn levels of ~0.35 μg/g and 1.8 μg/g (wet wt.) from prior studies in our lab (Lucchini et al., 2012), and a brain protein content of 115 mg protein/g brain (Banay-Schwartz et al., 1992), supporting both the relevance and translation of the AF5 cell study results to Mn exposures in intact organisms.

The Mn exposure levels that produced the GPP130 degradation response in AF5 cells were also 20- to 1000-fold lower than levels used in prior studies reporting sensitive cellular targets of Mn exposure. For example, studies in AF5 cells showed evidence of altered cellular metabolism, including increased intracellular GABA and disrupted cellular iron

homeostasis at Mn exposure levels as low as 25–50 μM Mn, or exposure levels ~50- to 100-fold higher than the lowest levels (0.54 μM Mn) causing GPP130 degradation in the present study (Crooks et al. 2007a,b; intracellular Mn levels following exposure were ~20 ng Mn/mg protein versus ~7 ng/mg protein in controls). In PC-12 cells, Mn exposure as low as 10 μM for 24 h were sown to disrupt cellular iron homeostasis (Kwik-Uribe et al. 2003, Kwik-Uribe and Smith, 2006; 10 μM exposure produced intracellular Mn levels of ~130 ng Mn/mg protein versus ~6 ng Mn/mg protein in controls). Tamm et al. (2008) reported apoptotic cell death in murine-derived multipotent neural stem cells exposed to 50 μM Mn. Most recently, Mukhopadhyay et al. (2010) showed GPP130 degradation in HeLa cells exposed to 100 μM to 500 μM Mn, or exposures ~200- to 1000-fold higher than the lowest levels used here; however, intracellular Mn levels were not reported in those studies, precluding direct comparison of Mn sensitivity between HeLa and AF5 cells. Collectively, these results underscore the highly sensitive nature of the GPP130 degradation response to Mn in comparison to other cellular targets of Mn exposure, and further substantiate a role for GPP130 in the transition from physiologic to supra-physiologic Mn homeostasis.

Currently, there is little known about the cellular responses and molecular mechanism(s) by which exposure to Mn over the transition between physiologic to supra-physiologic/toxic levels leads to cellular and neurological dysfunction. Our study addressed this knowledge gap by showing (i) GPP130 degradation is an early and sensitive cellular response to even very low Mn exposures, (ii) GPP130 protein appears to be robustly expressed in selective brain cells, and (iii) Mn exposure produces significant reductions in cellular GPP130 protein levels in a subset of brain cells, suggesting that cells within the brain differ in their GPP130 degradation response to Mn. While the implication of these results has yet to be determined, a recent study reported that the Mn-induced degradation of GPP130 blocked endosome to Golgi trafficking of Shiga toxin and caused its degradation in lysosomes, and mice exposed to elevated Mn were resistant to a lethal dose of Shiga toxin (Mukhopadhyay and Linstedt, 2012). Thus, further study is needed, including detailed analyses of cells in the brain that express significant levels of GPP130, to fully elucidate the role of GPP130 in cellular Mn homeostasis and cytotoxicity relevant to environmental exposures in humans.

ACKNOWLEDGMENTS

The authors thank T. Jursa, B. Powers, and S. Tabatabai for analytical assistance, M. Camps and C. Saltikov for comments on the manuscript, Benjamin Abrams at the UCSC Life Science Microscopy Center for microscopy support, and A. Linstedt and S. Mukhopadhyay for helpful discussions.

Contract grant sponsor: National Institutes of Health; Contract grant number: R01ES018990, R01ES019222.

REFERENCES

Aschner M, Erikson KM, Dorman DC. Manganese dosimetry: species differences and implications for neurotoxicity. Crit Rev Toxicol. 2005; 35:1–32. [PubMed: 15742901]

Banay-Schwartz M, Kenessey A, DeGuzman T, Lajtha A, Palkovits M. Protein content of various regions of rat brain and adult and aging human brain. Age. 1992; 15:51–54.

Bertinchamps AJ, Miller ST, Cotzias GC. Interdependence of routes excreting manganese. Am J Physiol. 1966; 211:217–224. [PubMed: 5911041]

Criswell SR, Perlmutter JS, Huang JL, Golchin N, Flores HP, Hobson A, Aschner M, Erikson KM, Checkoway H, Racette BA. Basal ganglia intensity indices and diffusion weighted imaging in manganese-exposed welders. Occup Environ Med. 2012; 69:437–443. [PubMed: 22447645]

Crooks DR, Welch N, Smith DR. Low-level manganese exposure alters glutamate metabolism in GABAergic AF5 cells. Neuro-Toxicology. 2007a; 28:548–554.

Crooks DR, Ghosh MC, Braun-Sommargren M, Rouault TA, Smith DR. Manganese targets m-aconitase and activates iron regulatory protein 2 in AF5 GABAergic cells. J Neurosci Res. 2007b; 85:1797–1809. [PubMed: 17469137]

Davidsson L, Lonnerdal B, Sandstrom B, Kunz C, Keen CL. Identification of transferrin as the major plasma carrier protein for manganese introduced orally or intravenously or after in vitro addition in the rat. J Nutr. 1989; 119:1461–1464. [PubMed: 2585137]

Da Silva, JJRF.; Williams, RJP. The Biological Chemistry of the Elements, The inorganic chemistry of Life. 2nd Ed.. Oxford England: Oxford University Press; 2001.

Garrick M, Dolan K, Horbinski C, Ghio A, Higgins D, Porubcin M, Moore E, Hainsworth L, Umbreit J, Conrad M. DMT1: A mammalian transporter for multiple metals. Biometals. 2003; 16:41–54. [PubMed: 12572663]

Gunter TE, Gavin CE, Aschner M. Speciation of manganese in cells and mitochondria: A search for the proximal cause of manganese neurotoxicity. Neurotoxicology. 2006; 27:765–776. [PubMed: 16765446]

Gwiazda RH, Lee D, Sheridan J, Smith DR. Low cumulative manganese exposure affects striatal GABA but not dopamine. NeuroToxicology. 2002; 23:69–76. [PubMed: 12164549]

Gwiazda RH, Kern C, Smith DR. Progression of neurochemical effects in different brain regions as a function of the magnitude and duration of manganese exposure. Toxicol Sci (Suppl). 2005; 84:122.

Gwiazda R, Lucchini R, Smith D. Adequacy and consistency of animal studies to evaluate the neurotoxicity of chronic low-level manganese exposure in humans. J Toxicol Environ Health A. 2007; 70:594–605. [PubMed: 17365613]

Gunshin H, Mackenzie B, Berger UV, Gunshin Y, Romero MF, Boron WF, Nussberger S, Gollan JL, Hediger MA. Cloning and characterization of a mammalian proton-coupled metal-ion transporter. Nature. 1997; 388:482–488. [PubMed: 9242408]

Keen, CL.; Lonnerdal, B.; Hurley, LS. Manganese. In: Frieden, E., editor. Biochemistry of the essential ultratrace elements. New York: Plenum Publishing; 1984. p. 89-132.

Kern CH, Stanwood GD, Smith DR. Preweaning manganese exposure causes hyperactivity, disinhibition, and spatial learning and memory deficits associated with altered dopamaine receptor and transporter levels. Synapse. 2010; 64:363–378. [PubMed: 20029834]

Kim E, Kim Y, Cheong HK, Cho S, Shin YC, Sakong J, Kim KS, Yang JS, Jin YW, Kang SK. Pallidal index on MRI as a target organ dose of manganese: structural equation model analysis. NeuroToxicology. 2005; 26:351–359. [PubMed: 15935207]

Kwik-Uribe CL, Reaney S, Zhu Z, Smith D. Alterations in cellular IRP-dependent iron regulation by in vitro manganese exposure in undifferentiated PC12 cells. Brain Res. 2003; 973:1–15. [PubMed: 12729948]

Kwik-Uribe C, Smith DR. Temporal responses in the disruption of iron regulation by manganese. J Neurosci Res. 2006; 83:1601–1610. [PubMed: 16568477]

Leitch S, Feng M, Muend S, Braiterman LT, Hubbard AL, Rao R. Vesicular distribution of secretory pathway Ca21 -ATPase Isoform 1 and a role in manganese detoxification in liver-derived polarized cells. Biometals. 2011; 24:159–170. [PubMed: 20981470]

Linstedt AD, Mehta A, Suhan J, Reggio H, Hauri HP. Sequence and overexpression of GPP130/GIMPc: Evidence for saturable pH-sensitive targeting of a type II early golgi membrane protein. Mol Biol Cell. 1997; 8:1073–1087. [PubMed: 9201717]

Lucaciu CM, Dragu C, Copaescu L, Morariu VV. Manganese transport through human erythrocyte membranes. An EPR Study. Biochimica et Biophysica Acta. 1997; 1328:90–98.

Lucchini R, Apostoli P, Perrone C, Placidi D, Albini E, Migliorati P, Mergler D, Sassine MP, Palmi S, Alessio L. Long-term exposure to “low levels” of manganese oxides and neurofunctional changes in ferroalloy workers. Neurotoxicology. 1999; 20(2–3):287–297. [PubMed: 10385891]

Lucchini, R.; Smith, DR.; Tjalkens, R. Manganese. In: Weiss, B., editor. Aging and vulnerability to environmental chemicals. Cambridge, UK: Royal Society of Chemistry Publishing; 2012.

Madejczyk B. The iron transporter ferroportin can also function as a manganese exporter. Biochim Biophys Acta. 2012; 1818:651–657. [PubMed: 22178646]

Montes S, Riojas-Rodríguez H, Sabido-Pedraza E, Ríos C. Biomarkers of manganese exposure in a population living close to a mine and mineral processing plant in Mexico. Environ Res. 2008; 106:89–95. [PubMed: 17915211]

Mukhopadhyay S, Bachert C, Smith DR, Linstedt AD. Manganese induced trafficking and turnover of the cis-golgi glycoprotein GPP130. MBoC. 2010; 21:1282–1292.

Mukhopadhyay S, Linstedt AD. Novel intra-golgi manganese sensor identifies hyperactive SPCA1 mutant that protects against manganese toxicity. Proc Natl Acad Sci USA. 2012; 108:858–863. [PubMed: 21187401]

Natarajan R, Linstedt AD. A cycling Cis golgi protein mediates endosome-to-golgi trafficking. Mol Biol Cell. 2004; 15:4798–4806. [PubMed: 15331763]

NRC. Guide for the care and use of laboratory animals. 8th edition. Washington, D.C: National Academy Press; 2011. National Research Council.

Paxinos, G.; Watson, C. The rat brain in stereotaxic coordinates. 4th ed.. San Diego: Academic Press; 1998.

Prohaska JR. Functions of trace elements in brain metabolism. Physiol Rev. 1987; 67:858–901. [PubMed: 3299411]

Puri S, Bachert C, Fimmel CJ, Linstedt AD. Cycling of early Golgi proteins via the cell surface and endosomes upon lumenal pH disruption. Traffic. 2002; 3(9):641–653. [PubMed: 12191016]

Racette BA, Aschner M, Guilarte TR, Dydak U, Criswell SR, Zheng W. Pathophysiology of manganese-associated neurotoxicity. NeuroToxicology. 2012; 4:881–886. [PubMed: 22202748]

Reaney SH, Bench G, Smith DR. Brain accumulation and toxicity of Mn(II) and Mn(III) exposures. Toxicol Sci. 2006; 93:114–124. [PubMed: 16740617]

Riccio A, Mattei C, Kelsell RE, Medhurst AD, Calver AR, Randall AD, Davis JB, Benham CD, Pangalos MN. Cloning and functional expression of human short TRP7, a candidate protein for store-operated Ca^{2+} influx. J Biol Chem. 2002; 277:12302–12309. [PubMed: 11805119]

Sepulveda MR, Vaoevelen J, Raeymaekers L, Mata AM, Wuytack F. Silencing SPCA1 (secretory pathway Ca2+ ATPase Isoform 1) impairs Ca2+ homeostasis in the golgi and disturbs neural polarity. J Neurosci. 2009; 29:12174–12182. [PubMed: 19793975]

Stanwood GD, Leitch DB, Savchenko V, Wu J, Fitsanakis VA, Anderson DJ, Stankowski JN, Aschner M, McLaughlin B. Manganese exposure is cytotoxic and alters dopaminergic and gabaergic neurons within the basal ganglia. J Neurochem. 2009; 110:378–389. [PubMed: 19457100]

Tamm C, Sabri F, Ceccatelli S. Mitochondrial-mediated apoptosis in neural stem cells exposed to manganese. Toxicol Sci. 2008; 101:310–320. [PubMed: 17977900]

Tan J, Zhang T, Jiang L, Chi J, Hu D, Pan Q, Wang D, Zhang Z. Regulation of intracellular manganese homeostasis by Kufor-Rakeb syndrome-associated ATP13A2 protein. J Biol Chem. 2011; 286:29654–29662. [PubMed: 21724849]

Yin Z, Jiang H, Lee EY, Ni M, Erikson KM, Milatovic D, Bowman AB, Aschner M. Ferroportin is a manganese-response protein that decreases manganese cytotoxicity and accumulation. J Neurochem. 2010; 112:1190–1198. [PubMed: 20002294]

Zota AR, Ettinger AS, Bouchard M, Amarasiriwardena CJ, Schwartz J, Hu H, Wright RO. Maternal blood manganese levels and infant birth weight. Epidemiology. 2009; 20(3):367–373. [PubMed: 19289966]

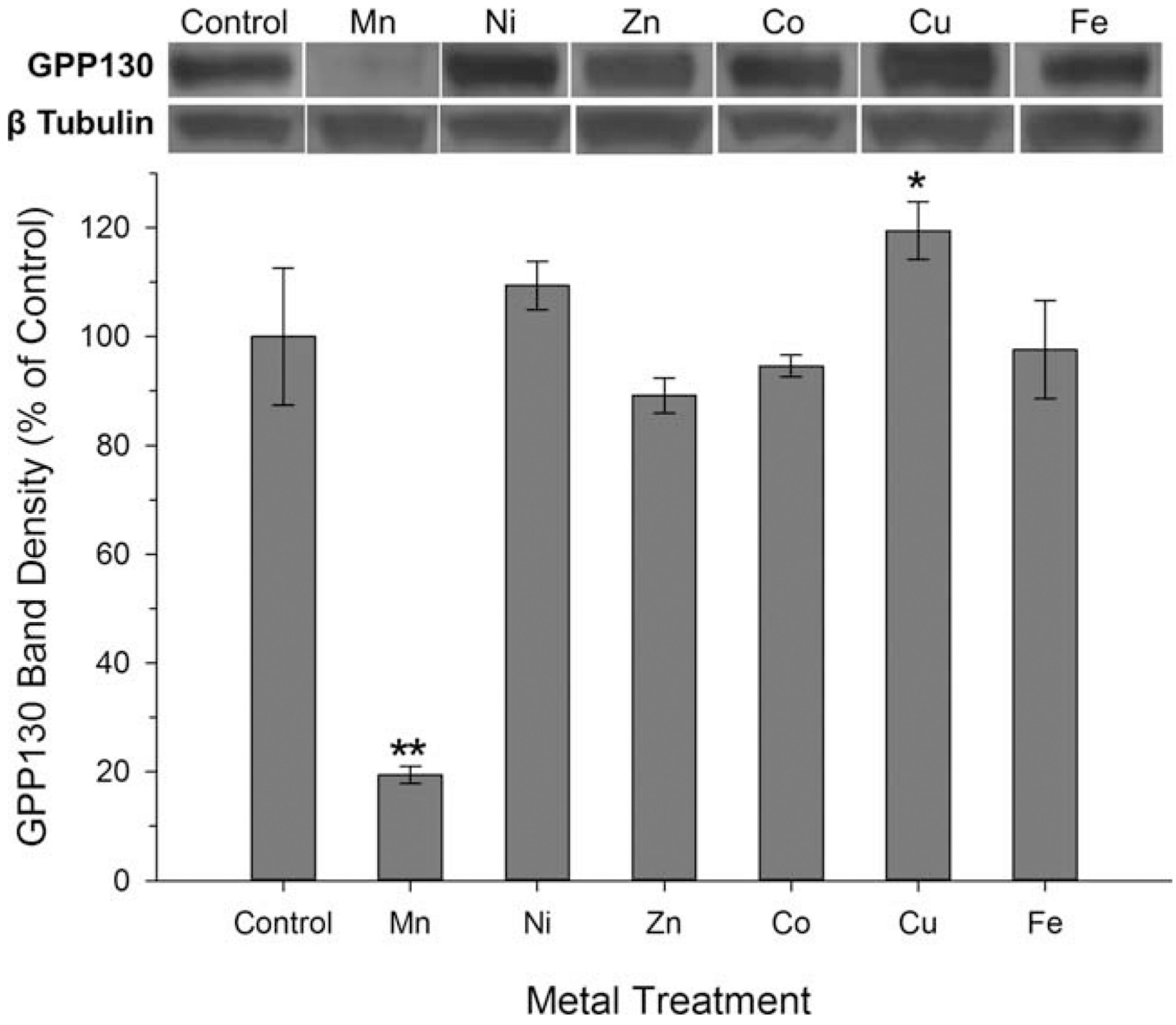

Fig. 1.

GPP130 degradation is Mn-specific. Cellular GPP130 levels were measured by Western blot in AF5 cells treated for 24 h with indicated metals (150 μM for all except Fe was 300 μM). Data are mean percent of control (±SD, *n*=3/treatment) from an experiment performed in triplicate. Asterisks indicate significantly different from control (**P*<0.05; ***P*<0.001), based on Dunnett's post hoc test. A representative Western blot for GPP130 and β-tubulin is shown above.

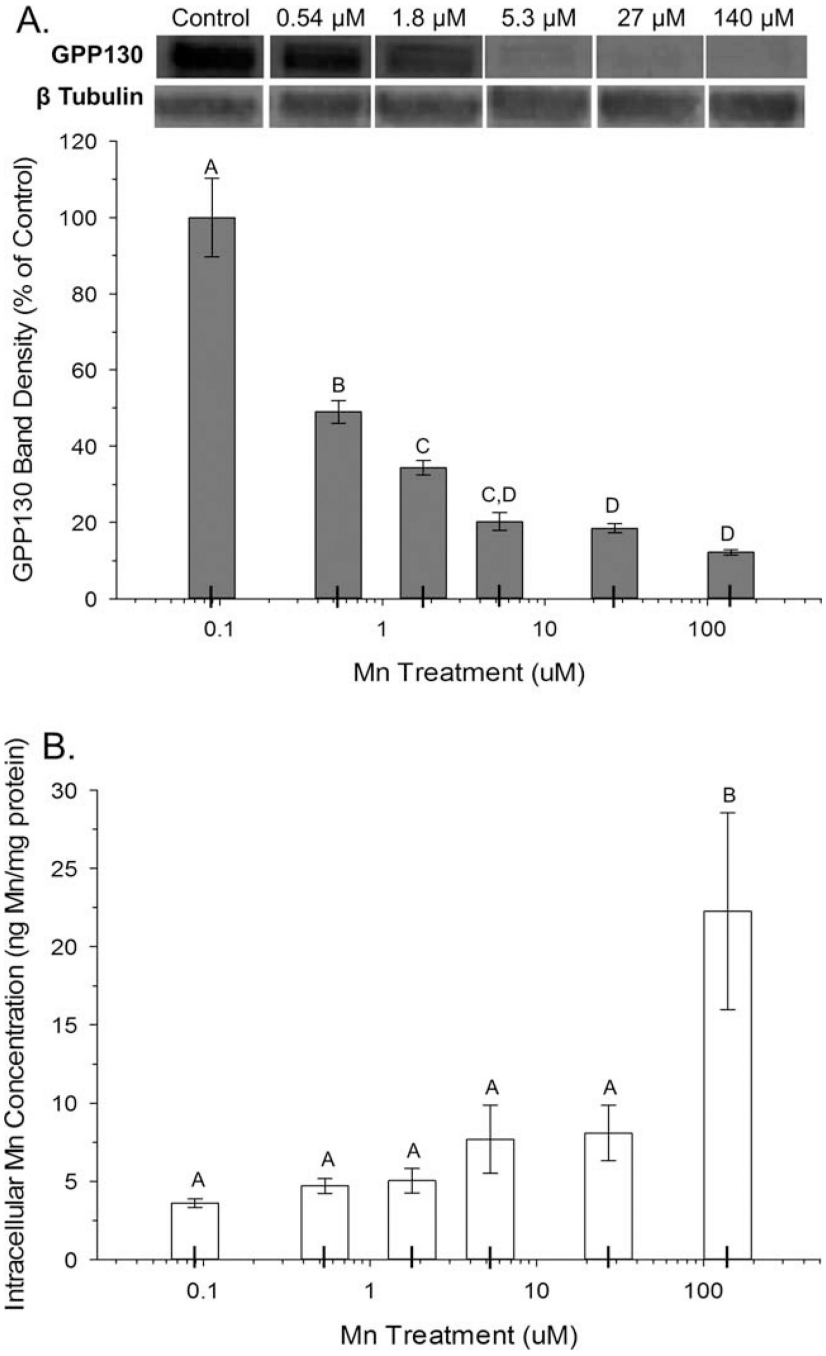

Fig. 2.

GPP130 degradation is sensitive to unmeasureable changes in intracellular Mn concentration. **A**: Cellular GPP130 levels were measured by Western blot and quantified as percent of control, in AF5 cells treated for 24 h with Mn at various concentrations (control (0.09), 0.54, 1.8, 5.3, 27, and 140 μM). **B**: Intracellular Mn concentrations in AF5 cells were measured by ICP-MS. All data are mean (±SD, *n*=3/treatment) from a representative experiment performed in triplicate. Superscript letters denote significant differences between

treatment groups; bars that do not share a common superscript are statistically different from one another ($P<0.05$), based on Tukey's post hoc test.

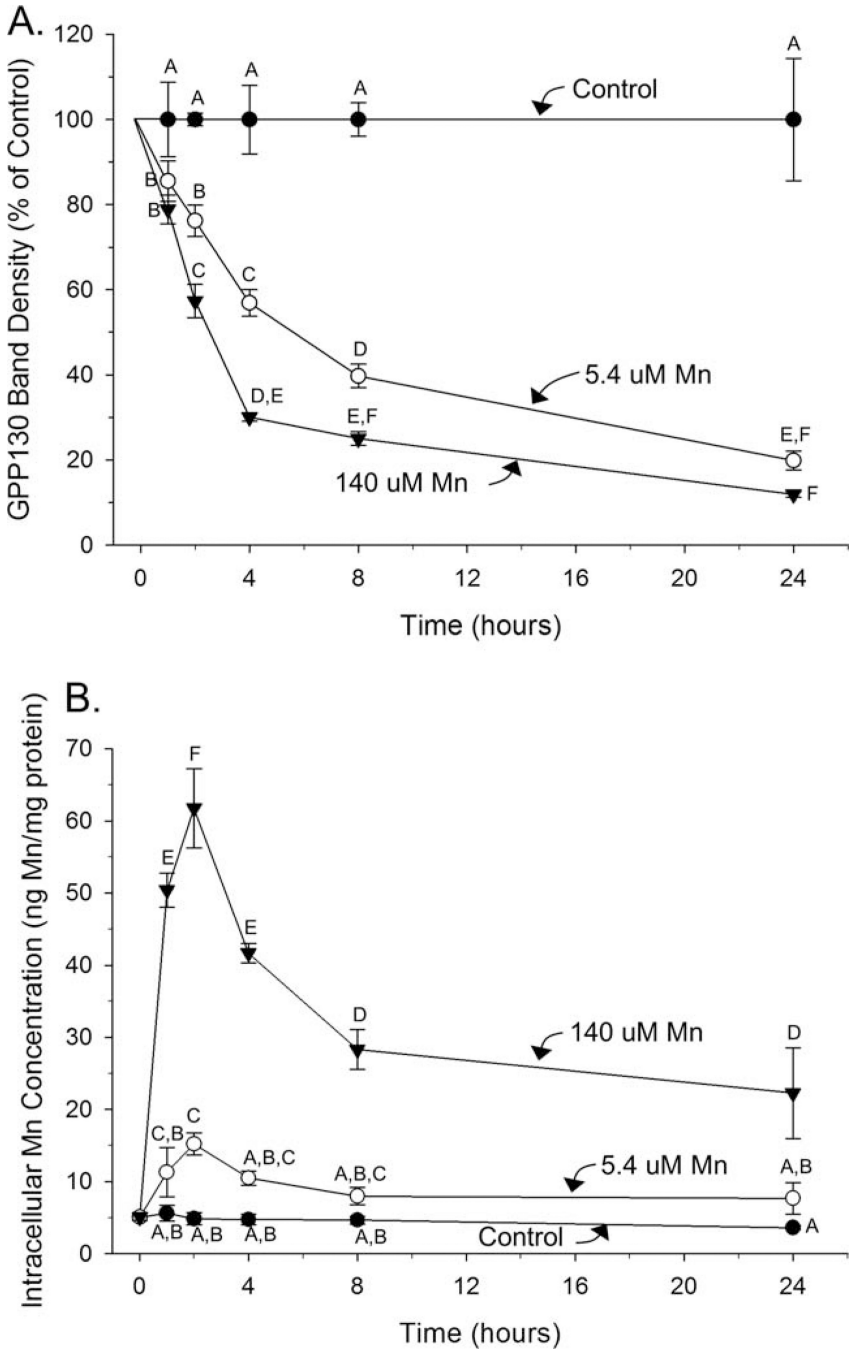

Fig. 3.

GPP130 degradation occurs rapidly with a parallel rapid increase then decrease in intracellular Mn concentrations over time. **A**: Cellular GPP130 levels by Western blot, a percent of control, in AF5 cells treated for 1, 2, 4, 8, or 24 h with control (0.09 μM), 5.4 μM, or 140 μM Mn. **B**: Intracellular Mn concentrations measured by ICP-MS in AF5 cells under the same conditions. Data are mean (±SD, *n*=3/treatment) from a representative experiment performed in triplicate. Superscript letters denote significant differences between treatment

groups; bars that do not share a common superscript are statistically different from one another ($P<0.05$), based on Tukey's post hoc test.

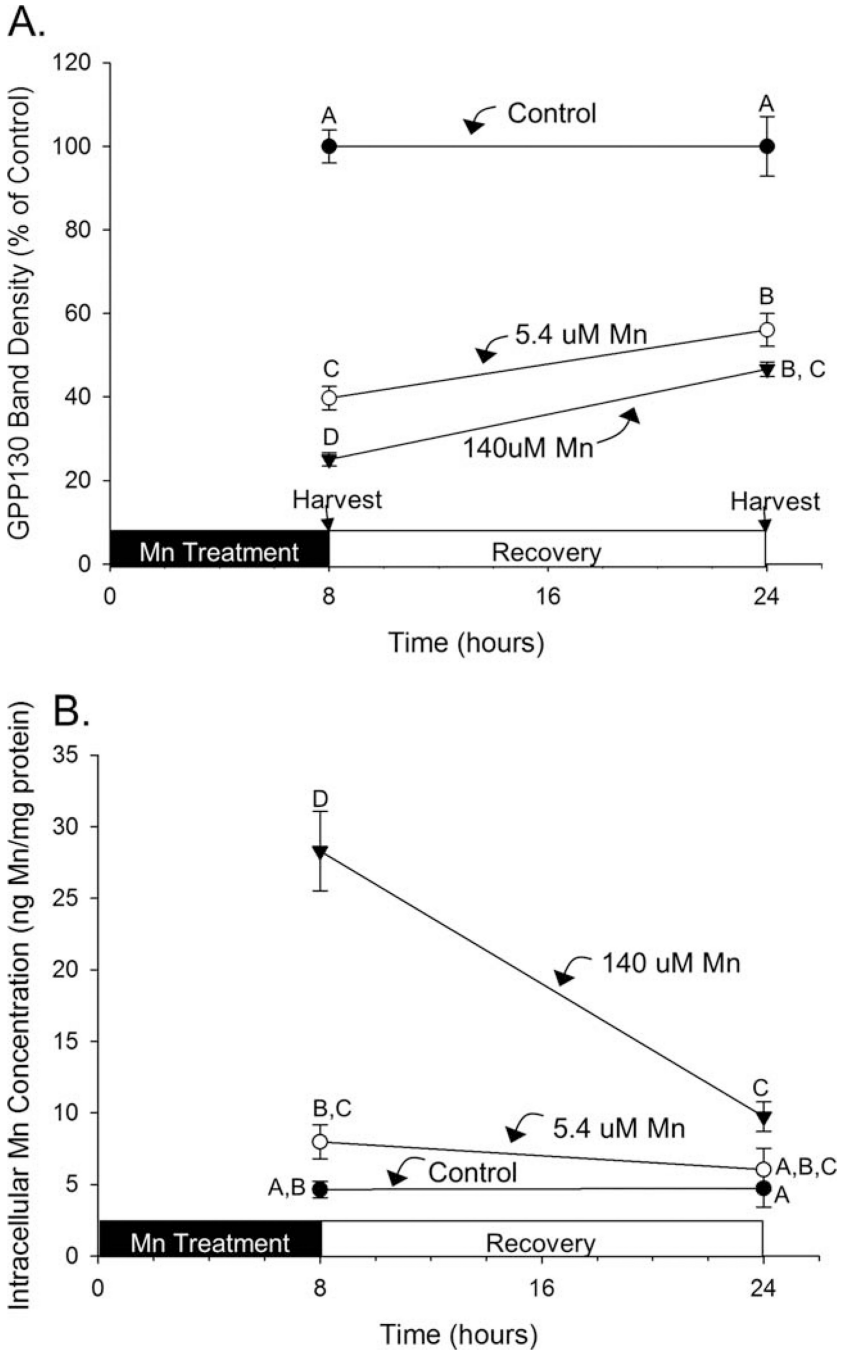

Fig. 4.

Recovery of cellular GPP130 levels is slower than the rate of disappearance. **A**: Cellular GPP130 levels by Western blot, as percent of control, in AF5 cells treated with control (0.09 μM), 5.4 μM, or 140 μM Mn for 8 h, followed by change to control medium for the subsequent 16 h. **B**: Intracellular Mn concentrations measured by ICP-MS in AF5 cells treated as above. Data are mean (±SD, *n*=3/treatment); data are from a representative experiment performed in triplicate. Superscript letters denote significant differences between

treatment groups; bars that do not share a common superscript are statistically different from one another ($P<0.05$), based on Tukey's post hoc test.

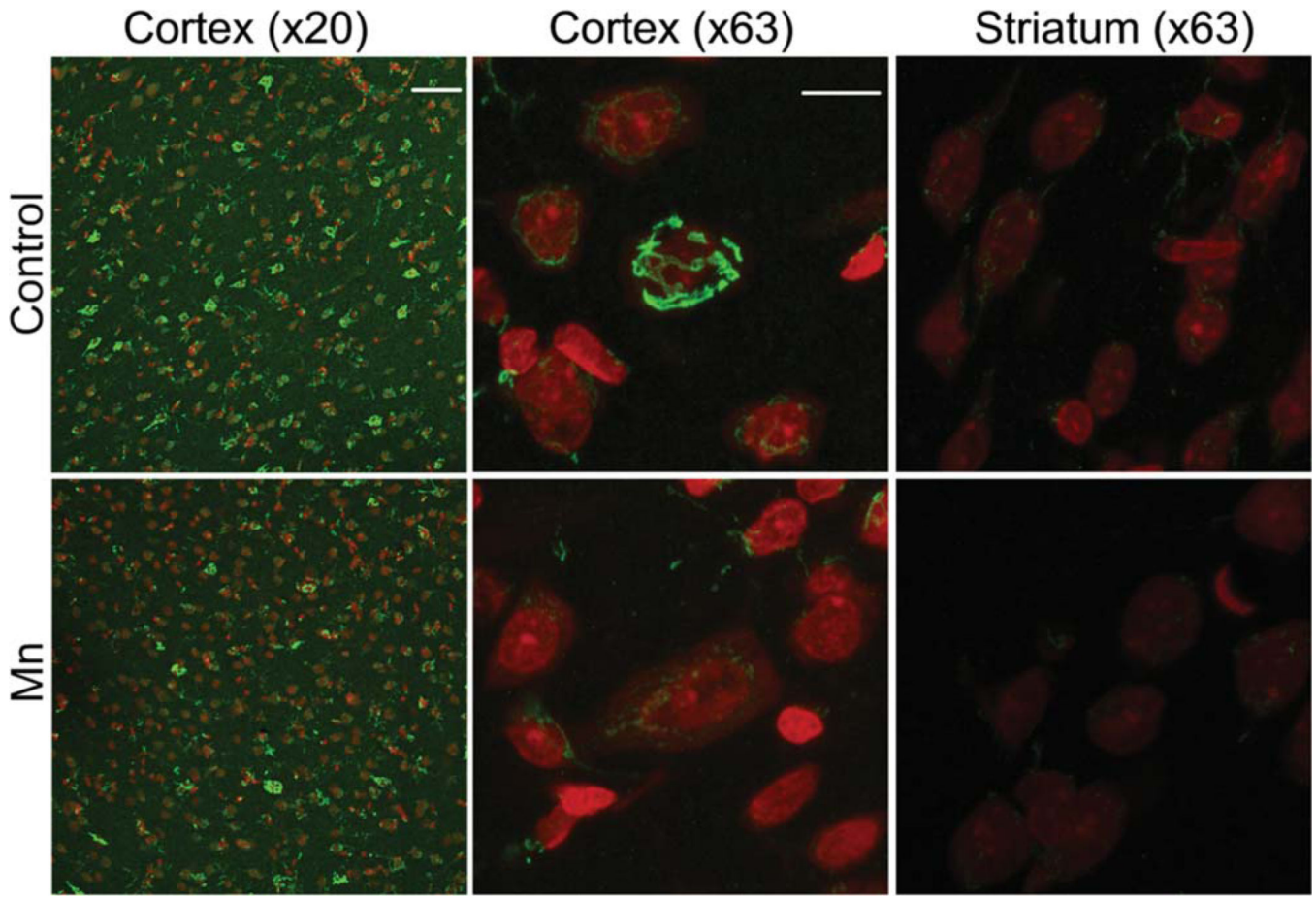

Fig. 5.

Mn exposure in rats reduces brain GPP130 levels in vivo. Representative IHC photomicrographs labeled with GPP130 (green) and Draq5 nuclear DNA stain (red) from cortex (S1 dysgranular zone, Bregma 0.48 mm) and dorsal striatum. Mn-exposed animals show an overall decrease in GPP130 levels in the cortex region of the brain compared to control animals. IHC slides were prepared and stained with three brain slices/animal/slide balanced by control and Mn treatment, and photographed at ×20 or ×63 magnification under defined illumination conditions (see text for details). Scale bar=50 μm for ×20, 10 μm for ×63.

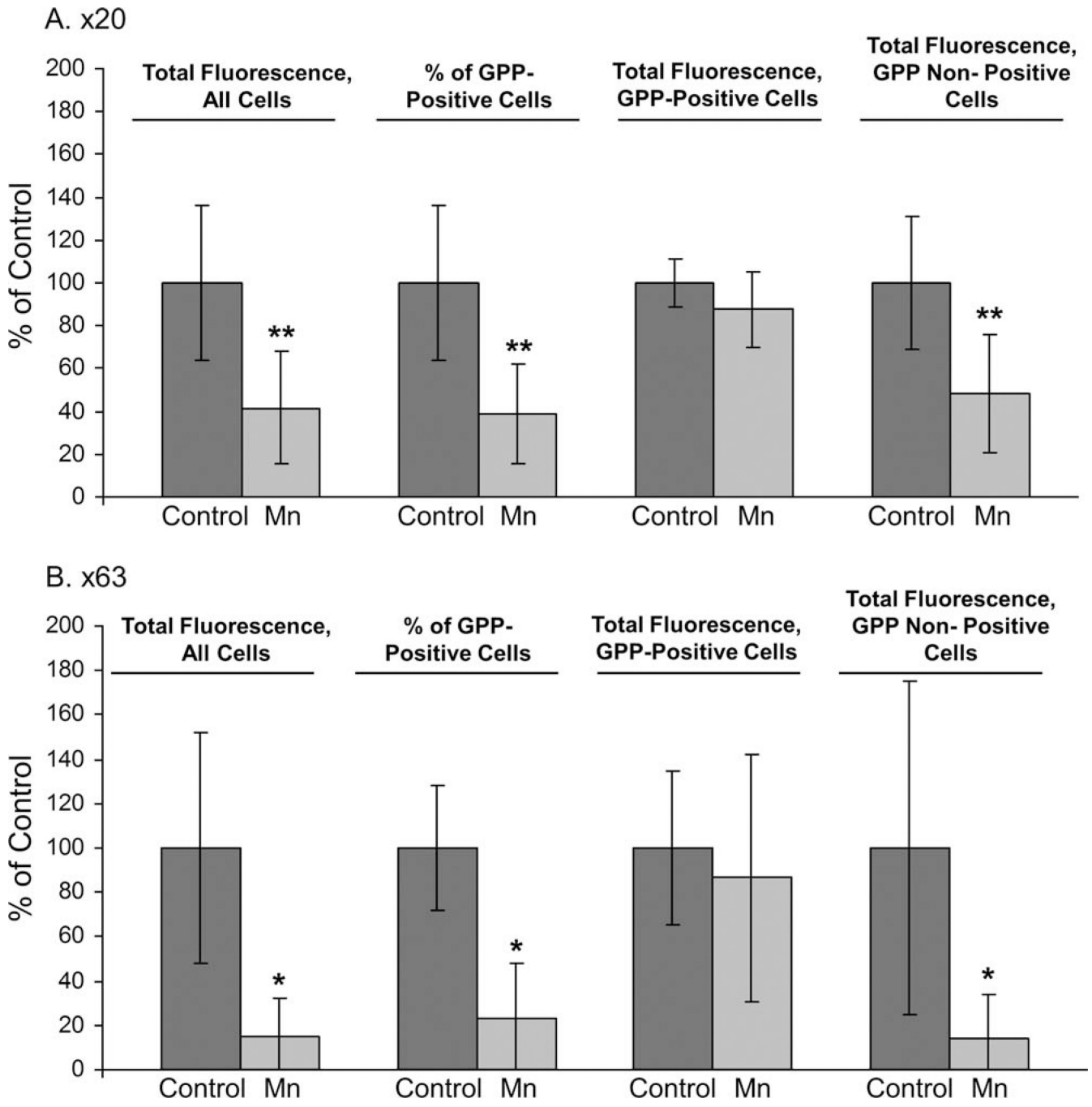

Fig. 6.

Mn exposure in rats reduces brain GPP130 levels in vivo primarily through reductions in GPP130-postive cells. Data quantified from fields at (**A**) ×20 magnification and (**B**) ×63 magnification, as follows: Total GPP130 fluorescence staining across all cells identified by the Draq5 nuclear DNA staining in the cortex (S1 dysgranular zone, Bregma 0.48 mm) of control and Mn exposed rats; percent of all cells identified that were GPP130-positive (see text for defined positive fluorescence threshold limits); total GPP130 fluorescence of GPP130-positive cells; and total GPP130 fluorescence in cells not identified as GPP130

positive (i.e., below the fluorescence threshold for GPP130-positive identification). Data are mean (±SD) expressed as percent of control group animals (see text for details). Asterisks indicate significantly different from respective control group (*P<0.05; **P<0.001, t-test).

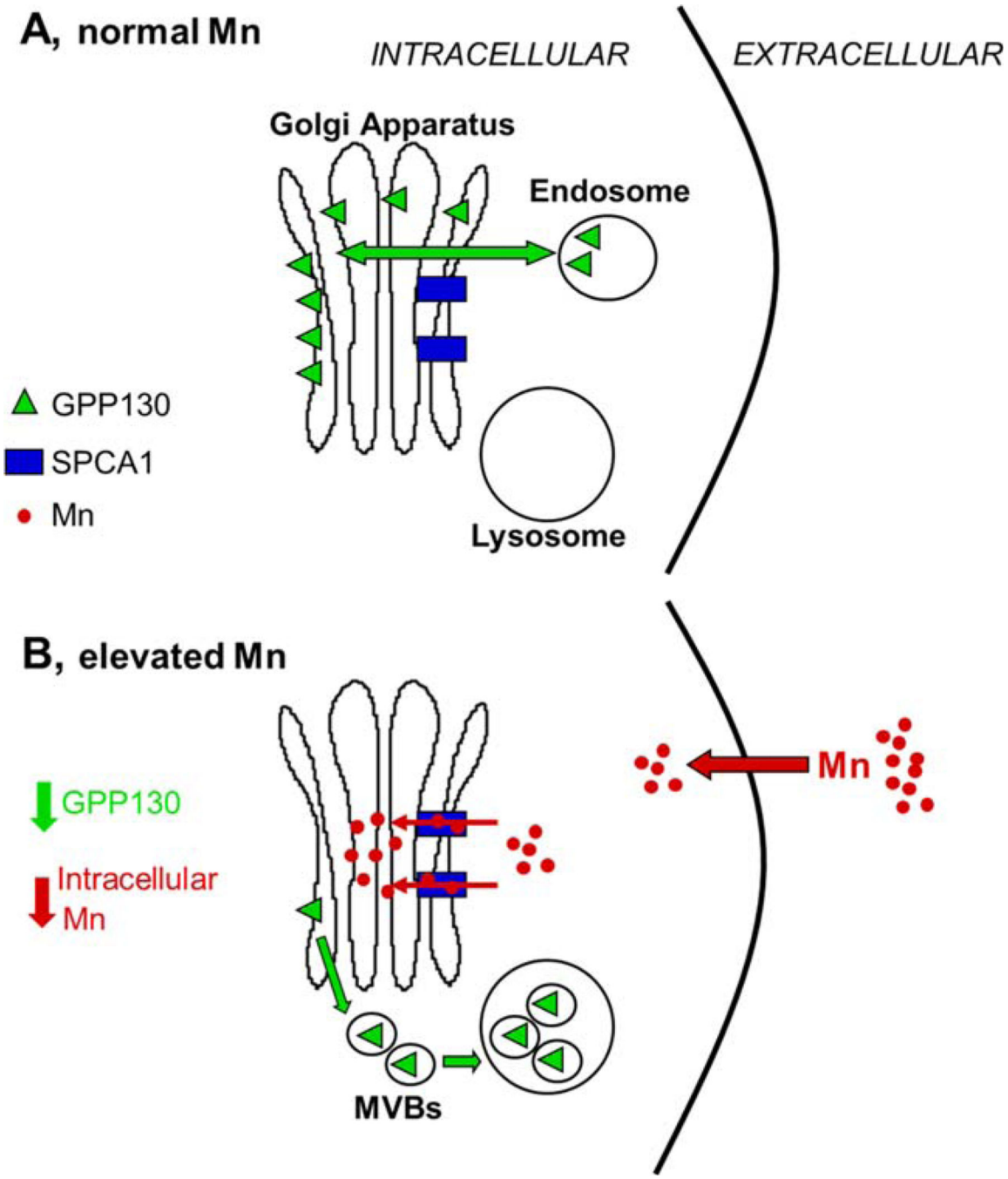

Fig. 7.

Cellular model for GPP130 in the presence of normal (**A**) and elevated (**B**) cellular Mn. A: GPP130 is localized to the cis-Golgi and participates in the bypass pathway by facilitating endosome to Golgi traffic. B: Upon elevated Mn exposure, Mn is transported into the Golgi lumen via SPCA1, which causes Golgi-localized GPP130 to traffic to MVBs and then to the lysosome, where it is ultimately degraded. As GPP130 degradation increases, the amount of

intracellular Mn decreases as well, suggesting that GPP130 may play a role in Mn homeostasis and susceptibility/resistance to elevated Mn exposure.

TABLE I

Total number of cells identified via Draq5 nuclear DNA staining, and the percent of GPP130-positive cells in cortex (S1 dysgranular zone, Bregma 0.48 mm) and dorsal striatum of Mn-treated rats, assessed at ×20 or ×63 magnification

		Average total # cells/field		Average %GPP positive cells	
Brain region	**Treatment**	**×20[a]**	**×63[b]**	**×20**	**×63**
Cortex	Control	602±88	12±2	23±12	34±11
	Mn	609±54	12±3	9±6**	7±7**
Striatum	Control	646±106	11±2	9±10	17±19
	Mn	672±58	10±2	5±5[c]	4±8[c]

Data are mean±SD; based on two microscopy fields per brain region (slice), six brain slices per animal, and three animals per treatment.

Data are mean±SD; based on 10 fields per brain region (slice) from one representative brain slice/animal/treatment.

Asterisks indicate significantly different from paired control (*P<0.05; **P<0.001, t-test).

TABLE II

Total GPP130 fluorescence across all cells identified via Draq5 nuclear DNA staining in the dorsal striatum of control and Mn exposed rats, percent of all cells identified that were GPP130-positive (see text for defined positive fluorescence threshold limits), and total GPP130 fluorescence of GPP130-positive cells, all quantified at ×63 magnification

Treatment	Total fluorescence, all cells[a]	% of GPP-positive cells	Total fluorescence, GPP-positive cells
Control	100±42	100±88	100±94
Mn	53±31**	23±55**	36±69[b]

Data expressed as percent of control group animals (see text for details).

Data are mean±SD, based on 10 fields per brain region (slice) from one representative brain slice/animal/treatment.

Asterisks indicate significantly different from paired control (*P<0.05; **P<0.001, t-test).